JOURNAL OF CATALYSIS **163,** 436–446 (1996)
ARTICLE NO. 0345

Roles of Carrier Gases on Deactivation and Coking in Zeolite Beta during Cumene Disproportionation

Wen-Hua Chen,*,† Ajit Pradhan,* Sung-Jeng Jong,* Ting-Yueh Lee,† Ikai Wang,† Tseng-Chang Tsai,‡
and Shang-Bin Liu*,[1]

**Institute of Atomic and Molecular Sciences, Academia Sinica, P.O. Box 23-166, Taipei, Taiwan 10764, Republic of China; †Department of Chemical Engineering, National Tsinghua University, Hsingchu, Taiwan 30043, Republic of China; and ‡Refining and Manufacturing Research Center, Chinese Petroleum Corporation, Chia-Yi, Taiwan 60038, Republic of China*

Received February 26, 1996; revised May 31, 1996; accepted May 31, 1996

The influence of carrier gases (N_2, H_2, He, and CO_2) on the catalytic activity, stability, and coke formation in zeolite beta during cumene disproportionation reaction is discussed. The reaction intermediates as well as the carbonaceous residues were characterized by ^{13}C NMR spectroscopy under proton cross-polarization and magic-angle spinning and by thermogravimetric method. The effects of carrier gas dilution on coke formation, catalyst deactivation, and product shape selectivity have also been examined by varying carrier gas (N_2) to reactant molar ratios (0.2–20). The amount of total coke decreases linearly with increasing N_2/cumene ratios above a value near 2. It is also found that the coke induced shape selectivity is notable only at extreme dilution. In the presence of various carrier gases, a notable decrease in catalytic activity has been found to obey the order $N_2 > H_2 > He > CO_2$, whereas a reverse order was observed for the catalytic stability. Moreover, the amount of coke deposit is found to decrease linearly with the kinetic diameter of the carrier gases. Hence, the incorporation of carrier gases resulted in a decrease in the amount of coke deposition which is mainly due to the transport of coke precursors and less bulky carbonaceous compounds (soft coke). Similarly, as proposed by the transition complex solvation model, the carrier gas molecules stabilize the biphenyl alkane reaction intermediates by van der Walls interactions and prevent them from further dissociation into product molecules. With the exception of H_2, the combination of the carrier gas transport effect and transition complex solvation model is used to describe the observed trends in the activity and stability of the catalyst.

INTRODUCTION

Although the study of diluent gas effect (DGE) during catalytic reaction was initiated over half a century ago, the subject has received little attention. In the early 1950s, some models for the DGE in heterogeneous catalytic systems were proposed. The major DGEs then considered were the variations in the activity of the reactants, product intermediates, or unstable complexes; the microscopic heat transfer effect; and transport of intermediate species in the catalyst phase (1–3), etc. Among them, models which attributed the DGE to either specific (2) or nonspecific (3) van der Waals interactions between the diluent gas and the activated complex states at the surfaces of the catalyst were found to be in good agreement with the experimental results.

In addition, the development of synthetic zeolites in catalytic cracking processes also led to a great advancement in catalyst design since 1950. However, deactivation of the catalyst by deposition of carbonaceous residues (coke) is inevitable during cracking reactions over zeolites (4–7). Hence, the control of coke formed during cracking reactions or retained during catalyst regeneration processes remains an important task. A practical way of easing the transport of the reactants and products through the zeolite catalyst and prolonging catalyst activity was to incorporate suitable diluent gases (or carrier gases) during the reaction. The carrier gas serves as a diluting medium to enhance the diffusivity and conductivity of the reactant and product molecules through zeolite intracrystalline pores or intercrystalline voids. The reactants, products, and reaction intermediates, if retained within the zeolite pores or channels, can affect the size/shape selectivity of the catalyst and hence are equally likely to enhance coke formation (8). Hence, the reaction chemistry of hydrocarbons in zeolite catalysts cannot be understood by monitoring the products alone.

Disproportionation of monoalkylbenzenes over zeolitic catalysts is one of the important reactions that possesses both academic and industrial interests. For the latter, the shape-selectivity characteristic of the zeolitic catalyst is also crucial in preparing valuable industrial raw materials such as *p*-dialkylbenzene isomers. The influences of carrier gases on catalytic activity and stability of zeolites during monoalkylbenzene disproportionation have been the subjects of several studies (9–15) in which hydrogen (H_2) and nitrogen (N_2) were the two most popular candidates for the study of DGE. For example, the effect of H_2 carrier gas on catalytic activity has been reported by Gnep and

---

[1] To whom correspondence should be addressed.

0021-9517/96 $18.00

Guisnet (11) for toluene conversion on mordenite zeolite and by Karge *et al.* (13) for ethylbenzene disproportionation on 0.2 wt% Pt/LaNaX zeolite. The decrease in catalytic activity is ascribed either due to the decrease in the concentration of intermediate benzylic carbocations (11, 12) or the decrease in Brønsted acidity (13, 14); both interpretations require the activation of molecular H_2.

Schulz-Ekloff *et al.* (15) investigated the variations of the catalyst conversion rate in the presence of different carrier gases. The authors disclosed that, under elevated pressures (>0.1 MPa), the degree of conversion during toluene disproportionation on H-ZSM-5 follows the order $H_2 < He < N_2 < Ar$. It was also concluded that the activity decreases with decreasing diameter of the carrier gas, except for N_2. The most severe deceleration of reaction rate was found in presence of H_2 and that hydrogen transfer activity which will also affect coke deposition can be promoted by O_2. The deceleration of the transalkylation rate was referred to the interactions between the carrier gas molecules with the hidden Lewis sites. The authors proposed that the carrier gas molecules may be polarized by the Lewis sites and consequently decrease the strength of neighboring Bønsted sites. On the other hand, in the case of inert carrier gas such as Ar or He, a direct shielding of catalytically active sites by the carrier gas molecules was proposed. However, both of the above interpretations require further support from experimental evidences.

Cumene disproportionation reaction is known as one of the potential routes for manufacturing *m*- and *p*-diisopropylbenzene (DIPB) isomers, two important intermediates for polymer industries. The same reaction has also been widely used as a probe for the structure (16) and acidity (17, 18) of zeolites. However, it is well known that the reaction mechanism and the catalytic activity are both strongly dependent on the morphology of zeolite (19). Owing to its highly siliceous nature and large (12-member rings) pores (20–24), zeolite beta has been shown to exhibit excellent activity, selectivity, and stability in monoalkylbenzene disproportionation (16, 25, 26) and therefore has practical potential in the production of DIPB. Some other potential applications of zeolite beta have been demonstrated, for example, in aromatic transalkylation (27–29), aliphatic hydrodewaxing (30, 31) and hydroisomerization (32), and cracking (33–35). However, besides its structural and thermal stability problems (36–38), zeolite beta catalyst is also vulnerable to deactivation by coking, especially during monoalkylbenzene disproportionation reactions (16, 26). A further understanding of the nature and mode of coke formation in zeolite beta during monoalkylbenzene disproportionation is therefore a demanding task.

In recent years, ^{13}C NMR in conjunction with proton cross-polarization (CP) and magic-angle spinning (MAS) has emerged as a powerful tool for studying the nature of the coke formed during hydrocarbon conversions over zeolite catalysts (39–41). Valuable information such as the state and mobility of the adsorbates and details of the related guest/host interactions can be obtained (42–48). In the present work, the nature and distribution of the coke formed in H-beta zeolite during cumene disproportionation reactions are investigated by ^{13}C CP-MAS NMR spectroscopy in conjunction with thermogravimetric analysis. The reaction was carried out under mild conditions (see below) to avoid unwanted cracking reactions. Two aspects of the DGE, namely (a) the nature of carrier gases and (b) the effects of dilution by nitrogen were selected to study the influence on activity and deactivation of zeolite beta during cumene disproportionation. The influences of various carrier gases, viz. N_2, H_2, He, and CO_2, were investigated at atmospheric pressure, while effects of N_2 dilution were carried out at high pressure (30 kg/cm^2) by varying the N_2/cumene molar ratio from 0.2 to 20. The coke-induced effects on shape selectivity are monitored by the ratio of *m*- to *p*-DIPB product isomers.

EXPERIMENTAL

Powdered, binderless zeolite beta ($SiO_2/Al_2O_3 = 25$) was obtained from Advchem Laboratory. Cumene solvent (A. R. Grade, Merck) was stored over activated 13X molecular sieves and was used without further purification. A stainless steel, continuous flow microreactor (15 mm i.d.) with a fixed bed of pressed and pelletized zeolite catalyst (10–20 mesh; ca. 4 g) was used for all reactions. The effects of various carrier gases were studied under the following conditions: temperature, 130°C; space velocity (WHSV) = 3.5 h^{-1}; carrier gas to cumene molar ratio, 2; pressure, 1 atm (0.101325 MPa). The effects of carrier gas dilution were studied with varied N_2/cumene ratios ranging from 0.2 to 20 under the following conditions: temperature, 135°C, WHSV = 3.5 h^{-1}, pressure, 30 kg/cm^2. These conditions were adopted such that the selectivity to disproportionation reaction can be kept more than 0.95 mol/mol and the initial conversion (time-on-stream (TOS) = 1 h) can be maintained at ca. 8–12 wt%. In a typical experiment, pressed and palletized zeolite beta catalyst was first activated in air at 450°C for 8 h; the system was then exposed to the desired carrier gas while bringing the temperature down to the reaction temperature. Upon completion of the experiment (TOS = 8 h), the system was purged with the carrier gas under the same experimental conditions for ca. 1 h before it was cooled down to room temperature (25°C). The detailed experimental and sampling procedures resemble those reported elsewhere (19). The compositions of the reactor effluents were analyzed by gas chromatography (Shimadzu Model GC-4A) using a packed column (5% SP-1200 + 1.75% Bentone 34 on 100/120 Supelcoport, 6 ft).

Thermogravimetric analysis (TGA) was conducted on a ULVAC TGD-7000 RH thermogravimeter. About 50 mg sample was used for the study and thermograms were recorded in presence of air with heating rate of 10°C min^{-1} from 30 to 800°C. The flow rate of air was maintained at 60 ml h^{-1}. Prior to the study, all fouled samples were stored over saturated NaCl solution in a dessicator to ensure complete hydration of each sample. Diffuse reflectance infrared (IR) spectra of selected samples were recorded with a Bomem Michelson spectrometer. Before recording the spectra, sample was dehydrated at 200°C for over 3 h.

The room temperature ^{13}C CP-MAS NMR spectra were obtained with proton decoupling on a Bruker MSL-500P spectrometer operating at resonance frequency 125.77 MHz. Typically, 5000–40,000 free induction decay (FID) signals were accumulated (depending on the amount of coke present in the sample) with a recycle delay of 1.0 s. The ^{13}C NMR chemical shifts were measured relative to tetramethylsilane (TMS).

In order to confirm the composition of the carbonaceous compounds formed during the reaction, selected samples were subjected to high temperature evacuation treatment. In a typical procedure, sample tube containing fouled sample was connected to a vacuum manifold and the sample temperature was raised slowly (1°C min^{-1}) to 210 or 270°C and then maintained at the respective temperature for at least 12 h under vacuum ($<10^{-5}$ Torr; 1 Torr = 133.3 Nm^{-2}). These temperatures were selected keeping in view of the boiling point of the major product, *m*-DIPB (204°C), and one of the possible components in the carbonaceous compounds, isopropylnaphthalene (267°C). After the evacuation treatment, the sample was then transferred to a 4-mm NMR rotor under nitrogen atmosphere before the ^{13}C CP-MAS NMR experiment.

The reproducibility of all catalytic and analytical experiments has been thoroughly checked. The possible experimental errors are reported in appropriate places.

RESULTS

Catalytic Activity

The catalytic data obtained from cumene disproportionation over zeolite beta, in the presence of various carrier gases, are summarized in Table 1 together with the physical properties of the carrier gases. The catalytic activities (presented in term of cumene conversions) against TOS of the reaction are shown in Fig. 1 for various carrier gases. The results indicate that, regardless of the type of carrier gas used, the activities of the catalyst decrease rapidly during the early stage (TOS ≤ 3 h) of the reaction and then gradually level off after TOS ≥ 6 h. The major products of the reaction are benzene and diisopropylbenzene isomers, as expected (16). According to our GC data, a traceable amount of ethylbenzene and *n*-propylbenzene were also found during the early stage (TOS < 2 h) of the reaction. It was found that, in the presence of various carrier gases, both the catalytic activities and the rates of disproportionation reaction at the steady state (Table 1) follow the order $N_2 > H_2 > He > CO_2$. The catalytic stability, on the other hand, was observed to follow the reverse order. The above observation is in variance with that reported by Schultz-Ekloff *et al.* (15). The authors observed a trend for toluene conversion during disproportionation reaction over H-ZSM-5 zeolite as $Ar > N_2 > He > H_2$. It should be pointed out that, in comparison, their reaction was done at much more severe conditions: temperature (300–320°C), WHSV (0.87 h^{-1}), and total pressure (0.1–1 MPa). Moreover, their reaction was carried out with different reactant and over a medium pore ZSM-5 zeolite.

TABLE 1

Physical Characteristics of Carrier Gases and Catalytic Data Obtained during Disproportionation of Cumene over Zeolite Beta

Carrier gases	N_2	H_2	He	CO_2
Physical characteristics[a]				
Electric dipole polarizability ($\times 10^{-24}$ cm^2)	1.740	0.804	0.205	2.911
Kinetic diameter (nm)	0.364	0.289	0.260	0.330
Catalytic data				
Rate at the steady state ($\times 10^{-3}$ mol h^{-1} g^{-1})	2.73	2.57	2.50	2.27
Conversion of cumene[b] (wt%)	10.5	10.2	9.3	8.1
m-/*p*-DIPB[b]	2.12	2.12	2.10	2.07
Total coke[c] (± 0.2 wt%)	8.6	9.7	9.5	8.4

[a] Ref. 61.

[b] Obtained at time-on-stream 1 h.

[c] Obtained after time-on-stream 8 h.

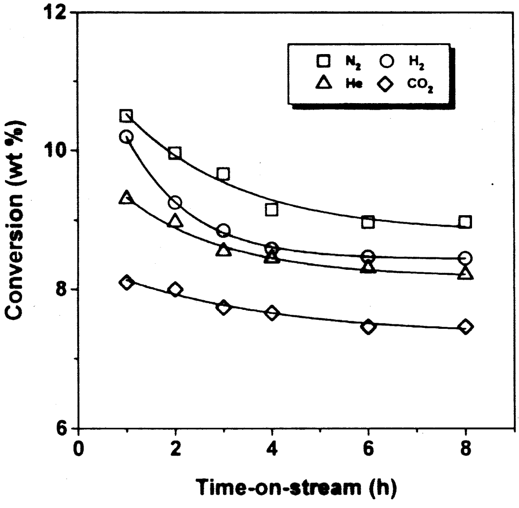

FIG. 1. The conversion of cumene against time-on-stream during disproportionation reaction over zeolite beta in the presence of various carrier gases; Reaction conditions: temperature, 130°C; N_2/carrier gas ratio, 2 mol/mol; WHSV, 3.5 h^{-1}; and pressure, 1 atm.

The effect of carrier gas dilution was studied by varying the N_2 carrier gas to reactant molar ratios. The experiments were carried out at a relatively higher pressure (30 kg/cm^2) and temperature (135°C) by which the reactant is in the liquid state and always saturates the surface of the catalyst. Under varied N_2/cumene ratios, the typical cumene conversion level was found to decrease from the initial value of ca. 13–15 wt% (TOS = 1 h) to ca. 5–7 wt% when reaching a TOS of 8 h. It is also found that variation in the flow rate of the carrier gas has no significant effect on the catalytic activity.

The distribution of DIPB isomers (the major products of the cumene disproportionation reaction), is highly shape-selective on zeolite catalysts (16, 49); a greater *m*- to *p*-DIPB product ratio is expected for zeolites with larger pore/channel openings. Besides the dependence on operating conditions, the observed *m*-/*p*-DIPB ratio should also depend on conversion level and nature and amount of total coke presenting in the catalyst. The ratio which normally increases with conversion level should eventually reach a thermodynamic equilibrium maximum of ca. 2.0. Moreover, at the same conversion level, the value of the *m*-/*p*-DIPB ratio can be used to monitor the coke-induced shape selectivity during the reaction (16, 49). As shown in Table 1, the *m*-/*p*-DIPB ratio obtained in the presence of various carrier gases are close to the equilibrium value of 2.0. Hence, no appreciable changes in the coke induced shape selectivity was found in the presence of different carrier gases. Figure 2 shows the variations of *m*-/*p*-DIPB ratio during cumene disproportionation reaction at various N_2 dilution levels. It is found that, at low N_2/cumene ratios, the *m*-/*p*-DIPB ratios decrease sharply with the level of cumene conversion (or degree of catalyst deactivation). However, the *m*-/*p*-DIPB ratio remains practically constant with respect to catalyst deactivation at higher N_2/cumene ratio. The results indicate that coke induced shape selectivity is significant only under extreme carrier gas dilution.

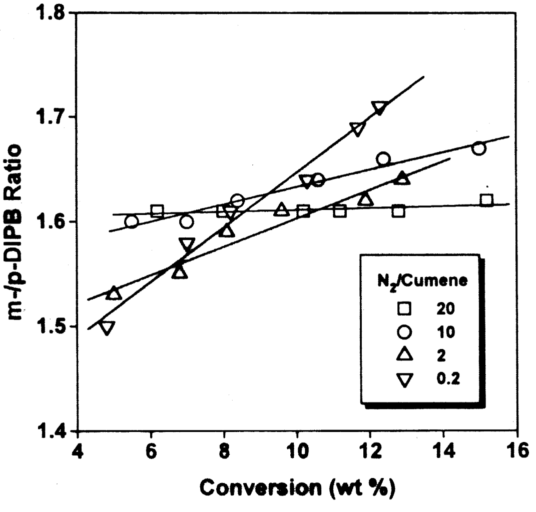

FIG. 2. Effects of cumene conversion on *m*- to *p*-DIPB ratio presented in the products at various N_2/cumene ratios during disproportionation reaction. Reaction condition: temperature, 135°C, WHSV, 3.5 h^{-1}; and pressure 30 kg/cm^2.

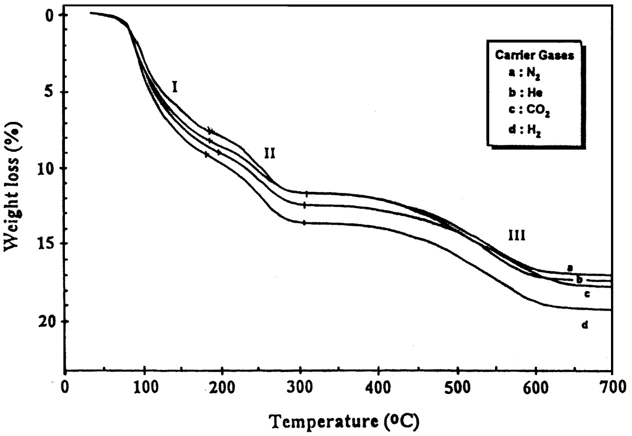

FIG. 3. Thermograms of the deactivated zeolite beta catalyst obtained in presence of various carrier gases.

Thermogravimetric Analysis

The thermograms of the deactivated catalysts under various carrier gases and N_2/cumene ratios (TOS = 8 h) are presented in Figs. 3 and 4, respectively. It appears that the observed thermogram can be roughly divided into three different temperature regions. The exact temperature range for each region varies slightly (ca. ±10°C) with the nature of different samples. Nonetheless, region I ($T < 180 \pm 10$°C) can be ascribed to the loss of water and volatile organic reactants, whereas regions II and III can be ascribed to the desorption of cokes (48). Normally, the less bulky (and hence more mobile) carbonaceous residues or physisorbed

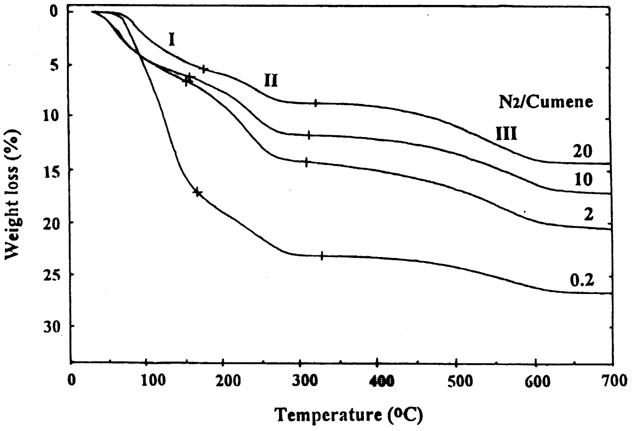

FIG. 4. Thermograms of the deactivated zeolite beta catalysts obtained under various N_2 dilutions.

products or side-products (hereafter termed as "soft cokes") should desorb at lower temperature (region II), whereas the more bulky carbonaceous compounds (termed as "hard cokes") will contribute to the weight loss at higher temperature (region III). However, it should also be noted that the "exact" amount of soft cokes (or hard cokes) cannot be readily determined from the weight loss in region II (or region III); some of the retained soft cokes (e.g., through oxidization processes) may eventually contribute to the weight loss in region III. Nevertheless, the above simplified differentiation provides us some crude information about the relative distribution of the soft cokes and hard cokes. The diverse nature of the thermograms indicates that the nature and dilution of carrier gases have significant influence on the composition and the concentration of coke residues.

^{13}C CP-MAS NMR Spectroscopy

The nature of the coke residues formed during the reaction in the presence of carrier gas was investigated by ^{13}C CP-MAS NMR spectroscopy. The ^{13}C NMR spectra obtained from the incorporation of various carrier gases and form various N_2 dilutions are presented in Figs. 5 and 6, respectively. All ^{13}C NMR spectra of the coked catalysts exhibit two distinct groups of resonance lines. The resonance lines located in the chemical shift ranges 0–50 and 110–150 ppm are assigned to aliphatics and aromatics, respectively (50–52). The lines of aliphatic species correspond to terminal methyl carbon (23 ppm) and penultimate methylene carbon (33 ppm) of the isopropyl group, while the lines of aromatic species correspond to substituted aromatic carbon (145–148 ppm) and nonsubstituted aromatic carbon (123–128 ppm).

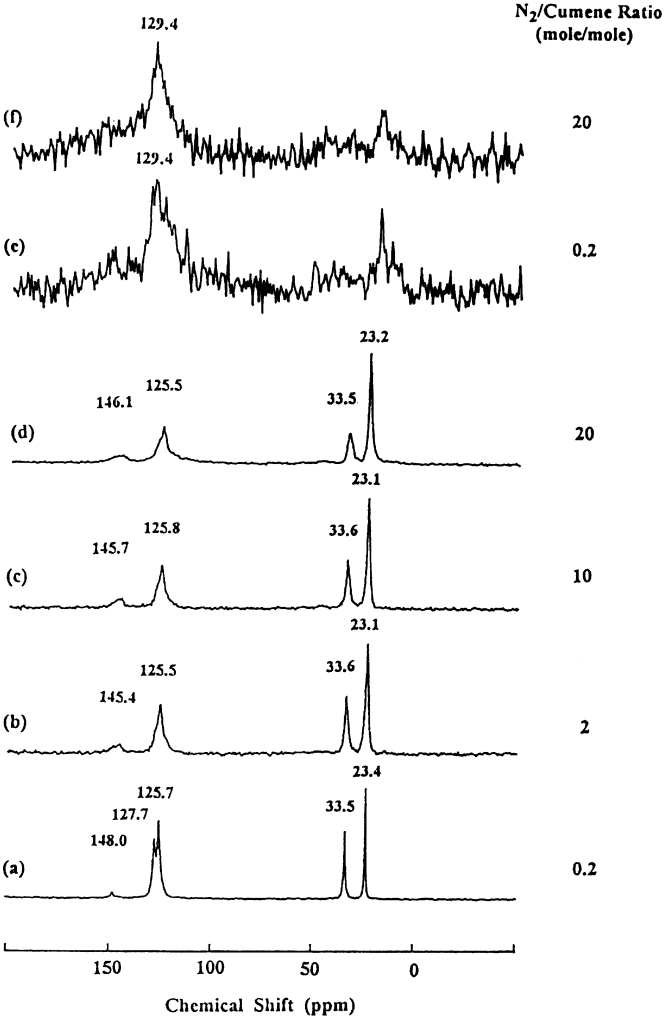

FIG. 6. The ^{13}C CP-MAS NMR spectra of the coked zeolite beta (a)–(d), at various N_2 dilutions; (e) and (f), the same samples originally prepared under respective N_2/cumene ratio of 0.2 and 20 were subjected to evacuation at 270°C for 12 h. All spectra were subjected to 30-Hz line-broadening.

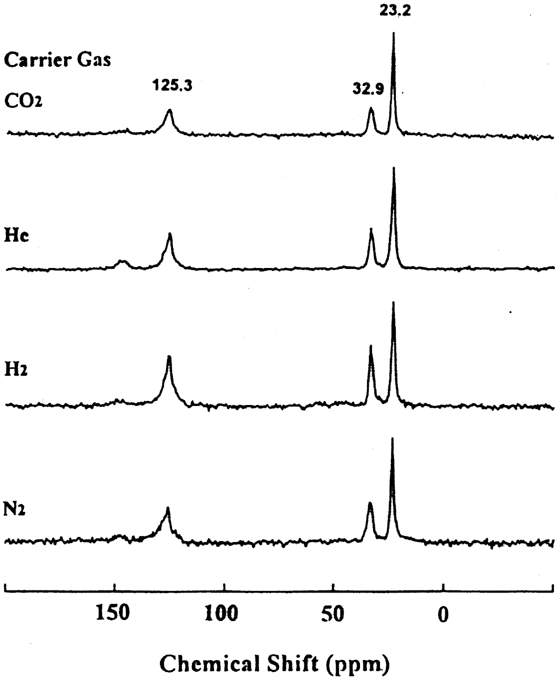

FIG. 5. The ^{13}C CP-MAS NMR spectra of the coked zeolite beta catalysts obtained after cumene disproportionation reactions in presence of various carrier gases. All spectra were subjected to 30-Hz line-broadening.

In order to identify the major constituent of the carbonaceous compounds, we performed separate ^{13}C NMR experiments in which the reactant (cumene) and the major product (*m*-DIPB) was individually introduced onto zeolite beta by means of physical mixing. When cumene was physically adsorbed on the surface of the zeolite crystallite, the ^{13}C NMR spectrum exhibits three distinct resonance lines at 147.3, 127.8, and 125.9 ppm and a small shoulder at 125.7 ppm in the aromatic region as shown in Fig. 7a,

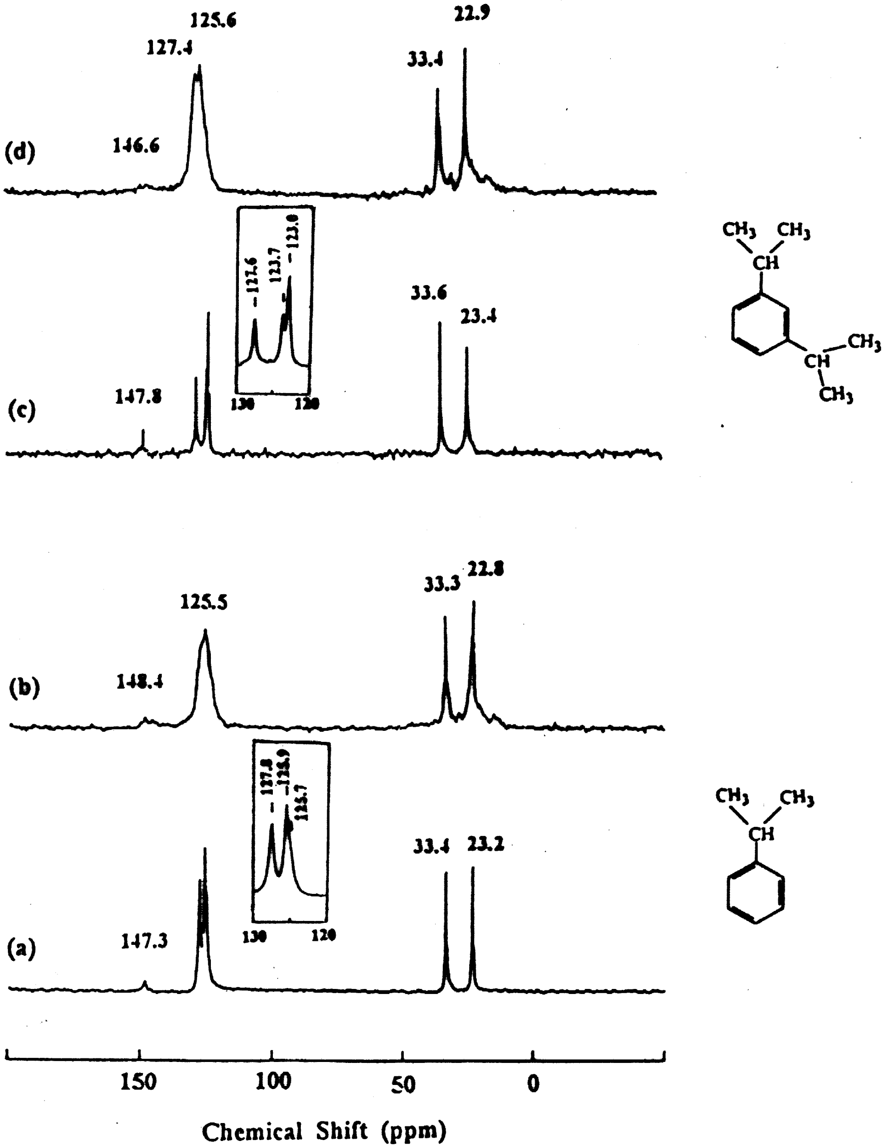

FIG. 7. The ^{13}C CP-MAS NMR spectra of (a) cumene, (c) *m*-DIPB physically adsorbed on zeolite beta; (b) and (d), after the respective samples (a) and (c) were heat treated at 200°C for 12 h. All spectra were subjected to 30-Hz line-broadening except for the blow-up regions.

whereas four distinct types of aromatic carbons (147.8, 127.6, 123.7, and 123.0 ppm) were observed in the case of *m*-DIPB (Fig. 7c). Spectra in Figs. 7b and 7d were obtained after the respective samples in Figs. 7a and 7c were heated at 200°C under vacuum to ensure a homogeneous intracrystalline adsorption (53, 54). The line broadening observed in Figs. 7b and 7d clearly indicate the decrease in adsorbate mobility as compared to the cases in Figs. 7a and 7c.

A detailed analysis of the ^{13}C NMR chemical shift and linewidth of the deactivated samples in presence of various carrier gases (Fig. 5) can be made by comparing with the results presented in Fig. 7. It is found that, in the presence of various carrier gases, the major constituents of the carbonaceous deposits are DIPB isomers, which are either trapped or physically adsorbed within the zeolite cages. A relatively small amount of tri-isopropylbenzene and/or alkylpolyaromatic species may also be present in the samples.

In the case of samples deactivated at various N_2 dilutions (Figs. 6a–6d), no appreciable changes in the chemical shift of the resonance peaks were observed, but the ^{13}C linewidths are found to increase with increasing N_2/cumene ratio. On comparing the spectra in Fig. 7d with those in Fig. 6a, it can be concluded that at low N_2/cumene ratio (0.2), the major constituent of the carbonaceous deposits formed over zeolite beta is DIPB isomers and there is nearly no trace of unreacted cumene. Moreover, based on the variations of spectral linewidth and relative line intensity in Figs. 6b–6d and 7d, it is indicative that, besides the DIPB isomers, more condensed carbonaceous compounds such as tri-isopropylbenzene and/or alkyl-polyaromatic species may also be formed and hence resulted in broad aromatic line at greater N_2 dilutions.

Removal of Soft Cokes in the Deactivated Zeolite Beta Catalysts

In order to gain further insight into the nature of cokes formed during the disproportionation reaction, the sample prepared with the two extreme N_2/cumene ratios (0.2 and 20) were dehydrated under vacuum at 270°C for 12 h; the respective ^{13}C CP-MAS NMR spectra are displayed in Figs. 6e and 6f. The purpose of the high temperature sample evacuation is to remove the retained DIPB isomers and volatile soft cokes while sustaining the high temperature reaction intermediates and hard cokes. In an earlier study, we demonstrated that such sample treatment does not change the nature of the condensed carbonaceous residues (48). After the treatment, samples were transferred into an air-tight NMR rotor under nitrogen atmosphere followed by ^{13}C CP-MAS NMR measurements. As evidenced by the broadening of the ^{13}C resonance (Figs. 6e and 6f), the carbonaceous species remaining in the catalyst are mostly bulky (less volatile) polyaromatics. The absence of the any additional features before and after the evacuation treatment indicates that there is no change or rearrangement in the nature of the carbonaceous compounds. It is noted that Magnoux *et al.* (52) have observed the formation of alkyl polyaromatics compounds having up to three aromatic rings at low temperature (120°C) during toluene disproportionation reaction.

The evacuation treatment of the deactivated catalysts obtained in the presence of various carrier gases were carried out at 210°C for 12 h. The resultant ^{13}C NMR spectra of fouled zeolite beta samples are presented in Fig. 8. That the spectra have poor sensitivity and much broader linewidths (compare to those before the treatment; cf. Fig. 5) indicates that most of the light aliphatic and soft cokes have been removed. It is notable that all spectra reveal the presence of a strong resonance peak at 126 ppm and a week shoulder peak at 145 ppm. Again, the broad peak at 126 ppm is assigned to nonsubstituted aromatics, whereas the peak at 145 ppm that has much weaker intensity and broader linewidth is ascribed as substituted aromatics. Moreover, for the deactivated samples originally obtained from reactions in presence of CO_2, N_2, and He, the ^{13}C spectra exhibit resonance lines at ca. 56, 33, and 23 ppm in the aliphatic region. Again, the lines at 33 and 23 ppm arise from penultimate methylene carbons and terminal methyl carbons, respectively (50–52). It is noted that, after the evacuation treatment, the enhancement of the line at 56 ppm (see Fig. 8) is accompanied by the suppression of the lines at 33 and 22 ppm (except for the case of H_2 carrier gas where the 56 ppm peak is practically invisible). The line at 56 ppm is *a priori* assigned to bridging carbon attaches to two phenyl and two methyl groups of the biphenyl reaction intermediate formed during the disproportionation reaction.

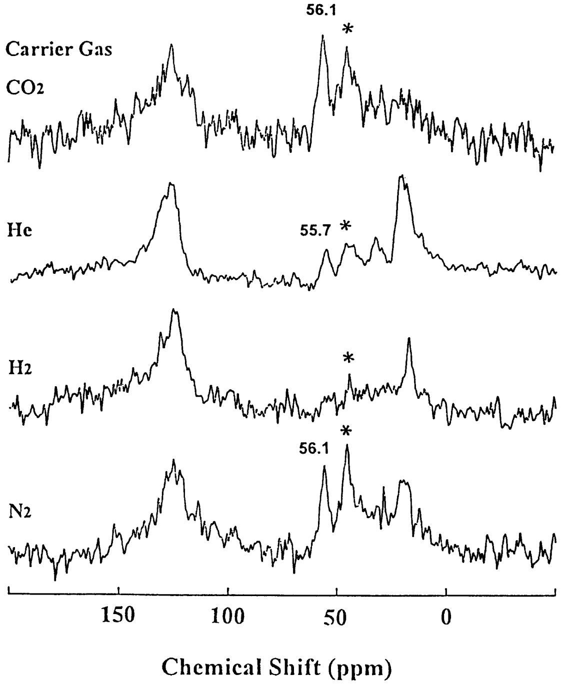

FIG. 8. The ^{13}C CP-MAS NMR spectra of the coked zeolite beta catalysts. In this context the samples in Fig. 3 were subjected to evacuation at 210°C for 12 h. All spectra were subjected to 80-Hz line-broadening. The peaks denoted by an asterisk represent spinning side-bands.

The ^{13}C NMR spectrum of the evacuated sample originally prepared in the present of H_2 carrier gas is rather different; it shows only a signal line (16 ppm) in the aliphatic region (Fig. 8). The line at 16 ppm is assigned to alkyl carbon of the partially hydrogenated polyaromatic species (50–52). This indicates that the mechanism of coke formation in the presence of H_2 carrier gas is markedly different from that under other carrier gases. The effects of H_2 on disproportionation reactions over zeolites have been reported (11–15). Schulz-Ekloff *et al.* (15) disclosed that the strongest deceleration of the toluene conversion over H-ZSM-5 zeolite is found in presence of H_2 carrier gas. The decrease in catalytic activity in presence of H_2 carrier gas has been ascribed due to the decrease in Brønsted acidity (13, 14) or the decrease in the concentration of intermediate benzylic carbocations (11, 12). Guisnet and co-worker further proposed that the interactions between the presenting H_2 molecule and the carbonium ion (reaction intermediates) will affect the equilibrium of carbonium ion formation and hence resulted in the decrease in toluene disproportionation rate over a mordenite catalyst (11, 12). Our ^{13}C NMR results also reveal that H_2 molecule may hydrogenate some of the reaction intermediates and/or coke compounds to form partially hydrogenated polyaromatic compounds.

IR Measurements

In pursuit of the reaction mechanism of cumene dispropotionation over zeolite beta in presence of various carrier gases, we continue our search for possible reaction intermediates. First, it has been found (55) that the formation of oxidized species is unlikely to occur during coking over zeolite catalyst because coke deposition normally involves reduction of hydrocarbon intermediates. If such species do exist, the ^{13}C resonance arises from the alkoxy functional group should appear at ca. 60 ppm (the exact chemical shift values vary with the number of presenting carbon atoms) on the observed NMR spectra (50–52). However, within the available signal-to-noise of our ^{13}C NMR spectra, no such resonance lines were observed from all the deactivated catalysts examined. Further confirmation of the reaction intermediates using diffuse reflectance IR technique has also been made. The absence of absorption peak (55, 56) at 1220–1250 cm^{-1} (correspond to C–O–C stretching band), 1720 cm^{-1} (C=O stretching), and 1460 and 1580 cm^{-1} (carboxylate species) in our IR spectra (not shown) indicate the absence of the corresponding species in the coke residues or reaction intermediates. Therefore, the only possible explanation for the ^{13}C resonance line at 56 ppm is due to the presence of biphenyl alkane intermediate; one of the components of the condensed coke or "hard coke." It is noted that biphenyl methane intermediates have been found in the coke residues formed during toluene disproportionation reaction over USY zeolite by Magnoux *et al.* using GC and MS techniques (52). Furthermore, the peak intensity for ^{13}C resonance at 56 ppm follows the trend for the corresponding carrier gas: $CO_2 > N_2 >$ He (see Fig. 8). This is in accordance with the transition complex solvation model to be described in the next section.

DISCUSSION

Interaction Mechanisms and Transition Complex Solvation Model

Two possible mechanisms which describe the interactions between the carrier gas molecules and the product molecules, reaction intermediates, or coke precursors can be envisaged, namely (a) carrier gas transport effect and (b) van der Waals interactions.

(a) Carrier gas transport effect. The formation of coke during hydrocarbon reactions over highly siliceous zeolite catalysts is the major source of catalyst deactivation. The carbonaceous residues mainly arise from product and/or side-product molecules which on retention within the zeolite channels or intracrystalline voids during reaction and hence may act as coke precursors (8). The coke precursor molecules may in turn decrease the catalytic activity by competitive poisoning of the acid sites or blocking the access of the reactant and product molecules to the acid sites (4–7). The effects of coking and deactivation in zeolite catalysts are also related to the guest/host interactions, e.g., mass transfer and diffusion limitations.

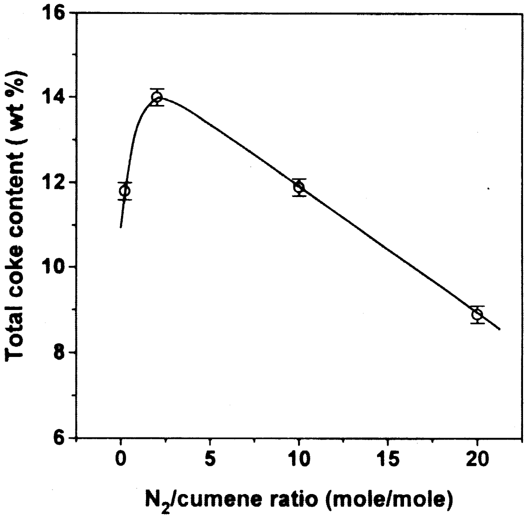

FIG. 9. Dependence of coke on various N_2 dilutions during cumene disproportionation reaction.

On the basis of the TGA data presented in Fig. 4, the variation of total coke content (calculated by the sum of weight loss in regions II and III of the thermograms) with the extent of N_2 dilutions is depicted in Fig. 9. Evidently the measured total coke content decreases linearly with increasing N_2/cumene ratio, except at very low N_2 dilution (i.e., N_2/cumene ratio = 0.2). The results therefore indicate that the incorporation of carrier gas has strong effect on formation and composition of cokes. A closer examination of the relative weight losses in the regions II and III of the thermograms (Fig. 4) reveal that while the amount of soft cokes desorbed in region II also decreases with increasing N_2/cumene ratio, the amounts of hard cokes remain practically unchanged. In comparison, the product DIPB isomers are more likely to be retained within the pore of zeolite beta at low N_2/cumene ratio than that at high N_2 dilutions. The retention of guest molecules within the pore of zeolite (host) hence resulted in the rapid catalyst deactivation and coke-induced shape selectivity observed in Fig. 2. In the extreme of N_2 dilution (N_2/cumene = 0.2), when the product molecules or coke precursors formed on the acid sites cannot be effectively removed from the zeolite intracrystalline voids, it is more likely to form soft cokes than the bulky polyaromatics hard cokes. In this context, the amount of total coke content is also low. On the other hand, a progressive increase in carrier gas concentration may prevent coke precursors from shielding of the active sites and thus sustaining the catalytic activity. However, the results obtained from the present study is in variance with that by Schultz-Ekloff *et al.* (15) who proposed shielding of active sites by carrier gas molecules.

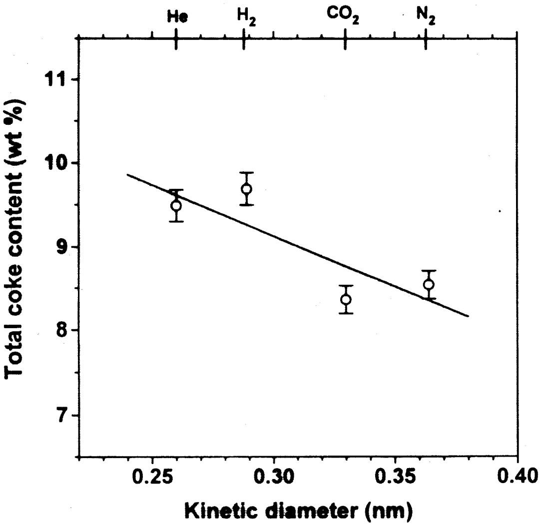

FIG. 10. Dependence of coke on the kinetic diameter of various carrier gases during cumene disproportionation reaction. The carrier gas to cumene ratios were kept constant (2.0).

The dependence of the coke content on the size of the carrier gases is shown in Fig. 10. It is found that, while the carrier gas to cumene molar ratios was remain constant (2.0), the amounts of total cokes present in the deactivated catalysts decreases linearly with increasing kinetic diameter of the carrier gas molecules. A careful analysis of the TGA data (Fig. 3) further reveals that the desorption of soft cokes is mainly responsible for the weight loss in regions II and III. The amounts of hard cokes deposited in the catalyst remain practically unchanged in the presence of various carrier gases. Hence, the transport ability of the carrier gas molecules therefore is nearly proportional to the kinetic diameter of the molecules.

However, though the removal of soft coke or coke precursors can be correlated to the decrease in catalytic activity (*vide supra*) in the order of carrier gases, $N_2 > H_2 >$ He, it fails to explain the low catalytic activity in the case of CO_2 which has a moderate molecular dimension. Thus, the interaction mechanism between the carrier gas molecules with the product molecules, reaction intermediates, and/or coke precursors cannot be interpreted by the physical effect alone.

(b) van der Waals interactions. In an earlier study, Tsai *et al.* (16) proposed that the zeolite beta catalyzes bimolecular (SN_2) reaction mechanism during disproportionation of cumene. The authors suggested that, cumene first forms a carbonium ion, then, a isopropyphenylcumene ion, and finally cracks into benzene and diisopropylbenzene molecules. To incorporate the influences of carrier gases on a reaction mechanism, an extended transition complex solvation model is proposed for cumene disproportionation reaction over zeolite beta, as depicted in Fig. 11. As proposed by Tsai *et al.* (16), cumene first forms a carbonium ion (Step 1) and then isopropylphenylcumene cation (Step 2), which was formed by bonding isopropylbenzene to isopropylbenzene carbonium ion. This carbonium ion then gets stabilized by resonance structures formed by Steps 4 and 5 and finally gets dissociated into benzene in Step 6 and diisopropylbenzene in Step 7. As these intermediates are highly reactive, formation of isopropylphenylcumene molecule from isopropylphenylcumene cation in Step 3 is not appreciable under normal circumstances. It may be noted that biphenyl methane type cations have been detected in zeolites mordenite, H-Y, and H-ZSM-5 by EPR and UV reflectance spectroscopy upon the sorption of toluene and biphenyl methane (57).

Recently, Xiong *et al.* (58) proposed a model for bimolecular mechanism in toluene disproportionation over H-ZSM-5 zeolite. Based on their results obtained from deuterium labeled compound, the authors concluded that the primary mechanism for the toluene disporportionation reaction involves the formation of biphenylmethane carbonium ion. When a small amount of diphenylemethane (which has been identified as precursor of benzylium chain transfer agents) was added to the reaction mixture, an acceleration in the reaction rate was observed. It was found that more than 98% of the added diphenylmethane was consumed during the reaction. Presumably, cumene should be a better reactant than toluene in studying the reaction mechanism for disproportionation reaction due to its relative ease in forming carbonium ion.

The transition complex solvation model is proposed according to the experimental results obtained from out ^{13}C NMR, IR, and TGA measurements. The model assumes that the carrier gas molecules may interact with biphenylalkane intermediates by van der Waals interactions and hence stabilize the carbonium ions. This ion–dipole type interaction should depend on the electric dipole polarizability of the carrier gas molecules. It is known (59) that the typical energy of such interaction is about 15 kJ mol^{-1}, which is lower than that of hydrogen bonding (ca. 20 kJ mol^{-1}). Quantum chemical calculations (60) also suggested that, during ion–dipole type interaction, stabilization of ions may take place by charge transfer from neutral atom/molecule to ions. Such charge transfer may occur during ion–atom or ion–molecule collisions.

Stabilization of carbonium ions slows down further dissociation of the biphenylalkane intermediates and ultimately resulted in a decrease in catalytic activity. A portion of isopropylphenylcumene cations may be stabilized by forming isopropylphenylcumene molecules during the process. Since such interaction depends upon electric dipole polarizability of the carrier gas molecules, the formation and presence of such reaction intermediates in the carbonaceous matter are appreciable only in the carrier gases that have higher electric dipole polarizability. As can be seen in

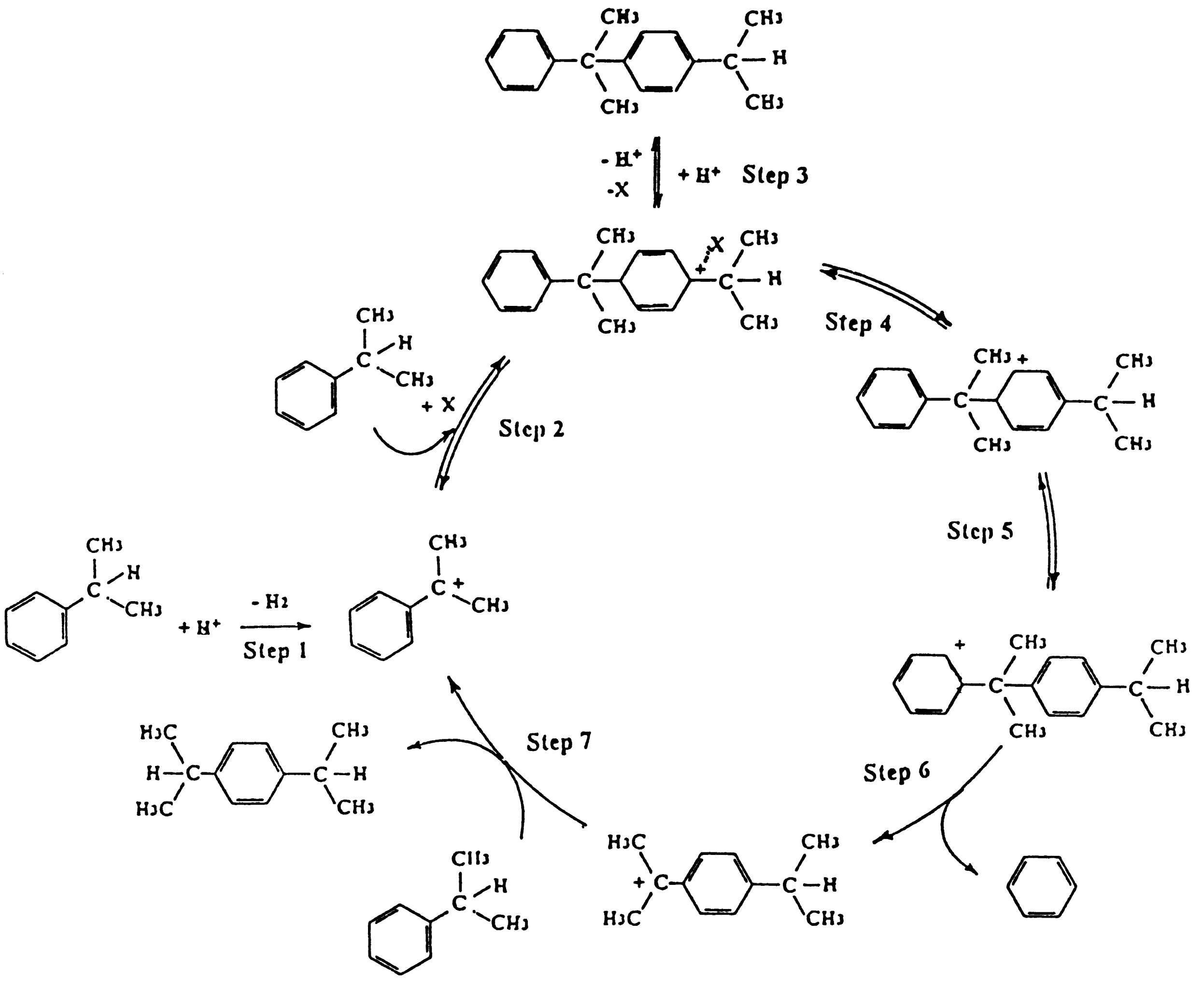

FIG. 11. Transition complex solvation model for cumene disproportionation reaction over zeolite beta in the presence of carrier gas (denoted by ×).

Table 1, while a CO_2 molecule possesses a moderate molecular size, its electric dipole polarizability is much higher than those of the other carrier gases included in this study. Thus, based on this transition complex solvation model, the catalytic activity should follow the trend of presented carrier gases, He $>$ N_2 $>$ CO_2, in accordance with the observed results. Thus, we conclude that the effects of carrier gases on catalytic activity can be interpreted only by the combination of physical (carrier gas transport effect) and van der Waals interactions.

CONCLUSIONS

In conclusion, a combination of physical and van der Waals interactions of carrier gas molecules with reaction intermediates and product molecules are used to explain the catalytic activity and stability of zeolite beta during the disproportionation of cumene in the presence of various carrier gases, viz. N_2, H_2, He, and CO_2. The ability of carrier gas molecules to remove carbonaceous matter and coke precursors from the zeolite cages (carrier gas transport effect) may be used to explain the trends in catalytic activity and stability of the catalyst in presence of various carrier gases except for CO_2. According to the transition complex solvation model, carrier gas molecule may stabilize the biphenyl alkane reaction intermediates by van der Waals interactions and prevents them from further dissociation into product molecules. The catalytic activity predicted by the model agrees with the experimental results. In the presence of H_2 carrier gas, the equilibrium for carbonium ion formation may be shifted by the H_2 molecules which may hydrogenate the reaction intermediates and/or coke compounds to from partially hydrogenated polyaromatic compounds.

The effects of carrier gas dilution have been studied with N_2 carrier gas by varying N_2/cumene molar ratios. It is found that the extent of carrier gas dilution has a strong influence on the formation of less bulky carbonaceous residues (soft cokes) but has little or no effect on the formation of bulky carbonaceous residues (hard cokes) except for system with very small N_2/cumene ratio. Moreover, the coke-induced selectivity is more notable for a system with greater N_2 dilution.

ACKNOWLEDGMENTS

We thank the National Science Council of Republic of China (NSC84-2113-M001-029 and NSC85-2113-M001-038) for support and for a postdoctoral research fellowship to A.P. We also thank the referees for valuable suggestions.

REFERENCES

1. Hudgins, R. R., and Silveston, P. L., *Catal. Rev. Sci. Eng.* **11**, 167 (1975).
2. Forestier, H., and Maurer, J., *C. R. Acad. Sci., Paris* **234**, 2196 (1952), and references therein.
3. McCabe, J. R., Grieger, R. A., and Eckert, C. A., *Ind. Eng. Chem.* **9**, 156 (1970), and references therein.
4. Bhatia, S., Beltramini, J., and Do, D. D., *Catal. Rev. Sci. Eng.* **31**, 431 (1989–1990).
5. Guisnet, M., Magnoux, P., *Appl. Catal.* **54**, 1 (1989).
6. Karge, H. G., *Stud. Surf. Sci. Catal.* **58**, 531 (1991).
7. Bibby, D. M., Howe, R. F., and McLellan, G. D., *Appl. Catal. A* **93**, 1 (1992).
8. Anderson, J. R., Chang, Y. F., and Western, R. J., *J. Catal.* **118**, 466 (1989).
9. Absil, R. P. L., Butt, J. B., and Dranoff, J. S., *J. Catal.* **92**, 187 (1985).
10. Bhavikath, S. S., and Patwardahan, S. R., *Ind. Eng. Chem. Prod. Res. Dev.* **20**, 102 (1981).
11. Gnep, N. S., and Guisnet, M., *Appl. Catal.* **1**, 329 (1981).
12. Guisnet, M., *J. Catal.* **88**, 249 (1984).
13. Karge, H. G., Sarbak, Z., Hatada, K., Weitkamp, J., and Jacobs, P. A., *J. Catal.* **82**, 236 (1983).
14. Karge, H. G., Wada, Y., Weitkamp, J., and Jacobs, P. A., *J. Catal.* **88**, 251 (1984).
15. Schulz-Ekloff, G., Jaeger, N. I., Vladov, C., and Petrov, L., *Appl. Catal.* **33**, 73 (1987).
16. Tsai, T. C., Ay, C. L., and Wang, I., *Appl. Catal.* **77**, 199 (1991).
17. Corma, A., and Wojciechoweski, B. W., *Catal. Rev. Sci. Eng.* **24**, 1 (1982).
18. Absil, R. P. L., Butt, J. B., and Dranoff, J. S., *J. Catal.* **85**, 415 (1984).
19. Tsai, T. C., and Wang, I., *J. Catal.* **133**, 136 (1992).
20. Wadlinger, R. L., Kerr, G. T., and Rosinski, E. J., U.S. patent 3,308,069 (1967).
21. Lok, B. M., Cannan, T. R., and Messina, C. A., *Zeolites* **3**, 282 (1983).
22. Newsam, J. M., Treacy, M. M. J., Koetsier, W. T., and De Gruyter, C. B., *Proc. R. Soc. London Ser. A* **420**, 375 (1988).
23. Treacy, M. M. J., and Newsam, J. M., *Nature (London)* **332**, 249 (1988).
24. Higgins, J. B., LaPierre, R. B., Schlenker, J. L., Rohrman, A. C., Wood, J. D., Kerr, G. T., and Rohrbaugh, W. J., *Zeolites* **8**, 446 (1988).
25. Ratnasamy, P., Bhat, R. N., Pokhriyal, S. K., Hegde, S. G., and Kumar, R., *J. Catal.* **119**, 65 (1989).
26. Wang, I., Tsai, T. C., and Ay, C. L., *Stud. Surf. Sci. Catal.* **75**, 1673 (1993).
27. Young, L. B., Eurpeon patent 30,084 (1981).
28. Wang, I., Tsai, T. C., and Huang, S. T., *Ind. Eng. Chem. Res.* **29**, 2005 (1990).
29. Innes, R. A., Zones, S. I., and Nacamuli, G. J., U.S. patent 4,891,458 (1990).
30. McGuiness, M. P., Mitchell, K. M., and Ware, R. A., U.S. patent 4,647,368 (1987).
31. Oleck, S. M., and Wilson, R. C., U.S. patent 4,568,655 (1986).
32. LaPierre, R. B., Partridge, R. D., Chen, N. Y., and Wong, S. S., U.S. patents 4,501,926 (1985) and 4,518,485 (1985).
33. Kennedy, C. R., and Ware, R. A., European patent application 186,447 (1986).
34. Chen, N. Y., Ketkar, A. B., Nace, D. M., Kam, A. Y., Kennedy, C. R., and Ware, R. A., European patent application 186,446 (1986).
35. Corma, A., Fornes, V., Monton, J. B., and Orchilles, A. V., *J. Catal.* **107**, 288 (1987).
36. Bourgeat-Lami, E., Massiani, P., Di Renzo, F., Fajula, F., and Des Courieres, T., *Catal. Lett.* **5**, 265 (1990).
37. Bourgeat-Lami, E., Massiani, P., Di Renzo, F., Espiau, P., and Fajula, F., *Appl. Catal.* **72**, 139 (1991).
38. Liu, S. B., Wu, J. F., Ma, L. J., Tasi, T. C., and Wang, I., *J. Catal.* **132**, 432 (1991).
39. Fyfe, C. A., "Solid State NMR for Chemists," Chap. 7. CFC Press, Guelph, Ontario, Canada, 1983.
40. Engelhardt, G., and D. Michel, D., "High-Resolution Solid-State NMR of Silicates and Zeolites," Chap. 7. Wiley, New York, 1987.
41. Haw, J. F., "NMR Techniques in Catalysis" (A. T. Bell and A. Pines, Eds.), Chap. 3. Dekker, New York, 1994.
42. Stocker, M., *Stud. Surf. Sci. Catal.* **85**, 429 (1994).
43. Meinhold, R. H., and Bibby, D. M., *Zeolites* **10**, 121 (1990).
44. Lange, J. P., Gutsze, A., Allgeier, J., and Karge, H. G., *Appl. Catal.* **45**, 345 (1988).
45. Barrage, M. C., Bauer, F., Ernst, H., Fraissard, J., Freude, D., and Pfeifer, H., *Catal. Lett.* **6**, 201 (1990).
46. Derouane, E. G., Gilson, J. P., and B. Nagy, J., *Zeolites* **2**, 42 (1982).
47. Ivanova, I. I., and Derouane, E. G., *Stud. Surf. Sci. Catal.* **85**, 357 (1994).
48. Liu, S. B., Prasad, S., Wu, J. F., Ma, L. J., Yang, T. C., Chiou, J. T., Chang, J. Y., and Tsai, T. C., *J. Catal.* **142**, 664 (1993).
49. Pradhan, A. R., and Rao, B. S., *J. Catal.* **132**, 79 (1991).
50. Stothers, J. B., "Carbon-13 NMR Spectroscopy," p. 90. Academic Press, New York, 1972.
51. Silverstein, R. M., Bassler, G. C., and Morvill, T. C., "Spectroscopic Investigation of Organic Compounds," Chap. 5. Wiley, New York, 1991.
52. Magnoux, P., Canaff, C., Machado, F., and Guisnet, M., *J. Catal.* **134**, 286 (1992).
53. Liu, S. B., Wu, J. F., Ma, L. J., Lin, M. W., and Chen, T. L., *Coll. Czech. Chem. Commun.* **57**, 718 (1992).
54. Liu, S. B., Ma, L. J., Lin, M. W., Wu, J. F., and Chen, T. L., *J. Phys. Chem.* **96**, 8120 (1992).
55. Datka, J., Sarbak, Z., and Eischens, R. P., *J. Catal.* **145**, 544 (1994).
56. Silverstein, R. M., Bassler, G. C., and Morrill, T. C., "Spectroscopic Investigation of Organic Compounds," Chap. 2. Wiley, New York, 1991.
57. Chen, F., Coudurier, G., and Naccache, C., *Stud. Surf. Sci. Catal.* **49**B, 1387 (1989).
58. Xiong, Y., Rodewald, P. G., and Chang, C. D., *J. Am. Chem. Soc.* **117**, 9427 (1995).
59. Atkins, P. W., "Physical Chemistry," p. 656. Oxford Univ. Press, Oxford, 1990.
60. Kaplan, I. G., "Theory of Molecular Interaction," p. 59. Elsevier, New York, 1986.
61. In "CRC Handbook of Chemistry and Physics" (C. W. Robert *et al.*, Eds.), Vol. 67, p. E-68. CRC Press, Boca Raton, FL, 1987.